

# Chapter 8

## Schawlow Townes limit and Spectral densities

### 8.1 The optical spectrum analyzer <sup>1</sup>

The most common OSAs for fiber optic applications use diffraction gratings as the basis for a tunable optical filter. Figure 8.1 shows what a diffraction-grating-based OSA might look like. In the monochromator, a diffraction grating (a minor with finely spaced corrugated lines on the surface) separates the different wavelengths of light. The diffracted light comes off at an angle proportional to wavelength. The result is similar to the rain bow produced by visible light passing through a prism. In the infrared, prisms do not work very well because the dispersion (in other words, change of refractive index versus wavelength) of glass in the Ito 2  $\mu\text{m}$  wavelength range is small.

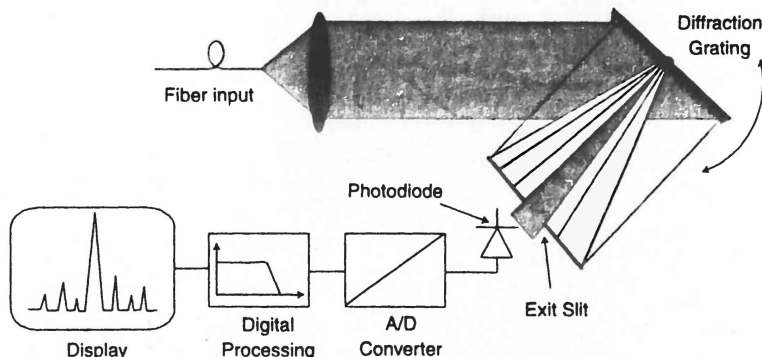


Figure 8.1: Concept of diffraction-grating-based OSA.

Diffraction gratings are used instead. They provide a greater separation of wavelengths allowing for better wavelength resolution. A diffraction grating is made up of an array of equidistant parallel slits (in the case of a transmissive grating) or reflectors (in the case of a reflective grating). The spacing of the slits or reflectors is on the order of the wavelength of the light for which the grating is intended to be used. The grating separates the different wavelengths of light because the grating lines cause the reflected rays to undergo constructive interference only in very specific directions. Only the wavelength that passes through the aperture reaches the photodetector to be measured. The angle of the grating determines the wavelength to which the OSA is tuned. The size of the input and output apertures together with the size of the beam on the diffraction grating determines the spectral width of the optical filter.

<sup>1</sup>Chapter 3 (Page 90 - 91) - Fiber optic test and measurement - Derickson, Dennis- New Jersey : Prentice Hall, 1998

## 8.2 Spontaneous emission noise and mode density <sup>2</sup>

Optical resonators, like their low-frequency, radio-frequency, and microwave counterparts, are used primarily in order to build up large field intensities with moderate power inputs. They consist in most cases of two, or more, curved mirrors that serve to “trap,” by repeated reflections and refocusing, an optical beam that thus becomes the mode of the resonator. A universal measure of this property is the quality factor  $Q$  of the resonator.  $Q$  is defined by the relation

$$Q = \omega \times \frac{\text{field energy stored by resonator}}{\text{power dissipated by resonator}} \quad (8.2.1)$$

As an example, consider the case of a simple resonator formed by bouncing a plane TEM wave between two perfectly conducting planes of separation  $l$  so that the field inside is

$$e(z, t) = E \sin \omega t \sin kz \quad (8.2.2)$$

And the average electric energy stored in the resonator is

$$\mathfrak{E}_{\text{electric}} = \frac{A\epsilon}{2T} \int_0^l \int_0^T e(z, t) dz dt \quad (8.2.3)$$

where  $A$  is the cross-sectional area,  $\epsilon$  is the dielectric constant, and  $T = 2\pi/\omega$  is the period. Using (8.2.2) we obtain

$$\mathfrak{E}_{\text{electric}} = \frac{1}{8} \epsilon E^2 V \quad (8.2.4)$$

where  $V = IA$  is the resonator volume. Since the average magnetic energy stored in a resonator is equal to the electric energy, the total stored energy is

$$\mathfrak{E} = \frac{1}{4} \epsilon E^2 V \quad (8.2.5)$$

Thus, recognizing that in steady state the input power is equal to the dissipated power, and designating the power input to the resonator by  $P$ , we obtain from (8.2.1)

$$Q = \frac{\omega E^2 V}{4P} \quad (8.2.6)$$

The peak field is given by

$$E = \sqrt{\frac{4QP}{\omega \epsilon V}} \quad (8.2.7)$$

### Mode Density in Optical Resonators

The main challenge in the optical frequency regime is to build resonators that possess a very small number, ideally only one, high  $Q$  modes in a given spectral region. The reason is that for a resonator to fulfill this condition, its dimensions need to be of the order of the wavelength.

Mode control in the optical regime would thus seem to require that we construct resonators with volume  $\sim \lambda^3$  ( $\sim 10^{-12} \text{ cm}^3$  at  $\lambda = 1\mu\text{m}$ ). This is not easily achievable. An alternative is to build large ( $L \gg \lambda$ ) resonators but to use a geometry that endows only a small fraction of these modes with low losses (a high  $Q$ ). In our two-mirror example, any mode that does not travel normally to the mirror will “walk off” after a few bounces and thus will possess a low  $Q$  factor. We will show later that when the resonator contains an amplifying (inverted population) medium, oscillation will occur preferentially at high  $Q$  modes, so that the strategy of modal discrimination by controlling  $Q$  is sensible. We shall also find that further modal discrimination is due to the fact that the atomic medium is capable of amplifying radiation only within a limited frequency region so that modes outside this region, even if possessing high  $Q$ , do not oscillate.

One question asked often is the following: Given a large ( $L \gg \lambda$ ) optical resonator, how many of its modes will have their resonant frequencies in a given frequency interval, say, between  $\nu$  and  $\nu + \Delta\nu$ ? To answer this problem, consider a large, perfectly reflecting box resonator with sides,

<sup>2</sup>Chapter 4 (Page 121 - 125) - Optical Electronics in Modern Communications- Fifth Edition - Amnon Yariv - Oxford University Press, 1997

$a, b, c$  along the  $x, y, z$  directions. Without going into modal details, it is sufficient for our purpose to take the amplitude field solution in the form

$$E(x, y, z) \propto \sin k_x x \sin k_y y \sin k_z z \quad (8.2.8)$$

(Resonators of different shapes will differ in detail, but for large,  $L \gg \lambda$ , resonators, the results are similar.)

$$k_x^2 + k_y^2 + k_z^2 = \left( \frac{\omega}{c} n \right)^2 \quad (8.2.9)$$

For the field to vanish at the boundaries, we thus need to satisfy

$$k_x = \frac{r\pi}{a}, k_y = \frac{s\pi}{b}, k_z = \frac{t\pi}{c} \quad r, s, t \text{ any integers} \quad (8.2.10)$$

With each such mode, we may thus associate a propagation vector  $\mathbf{k} = \hat{x}k_x + \hat{y}k_y + \hat{z}k_z$ . The triplet  $r, s, t$  defines a mode. Since replacing any integer with its negative does not, according to Equation (8.2.8), generate an independent mode, we will restrict, without loss of generality,  $r, s, t$  to positive integers. It is convenient to describe the modal distribution in  $\mathbf{k}$  space, as in Figure 8.2. Since each (positive) triplet  $r, s, t$  generates an independent mode, we can associate with each mode an elemental volume in  $\mathbf{k}$  space.

$$V_{mode} = \frac{\pi^3}{abc} = \frac{\pi^3}{V} \quad (8.2.11)$$

where  $V$  is the physical volume of the resonator. We recall that the length of the vector  $\mathbf{k}$  satisfies Equation (8.2.10), rewritten here as

$$k(r, s, t) = \frac{2\pi\nu(r, s, t)}{c} n \quad (8.2.12)$$

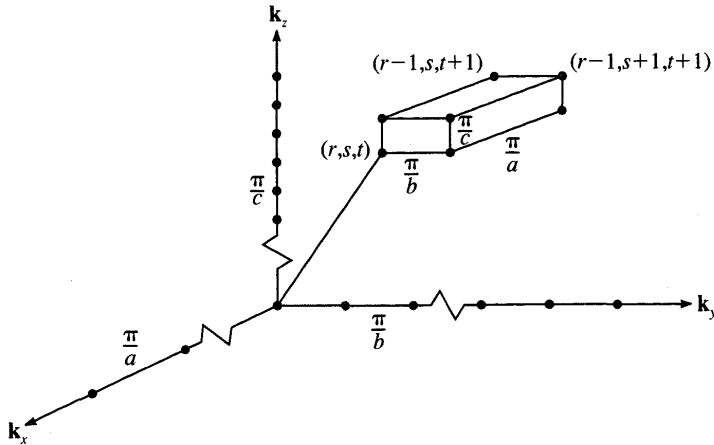


**Figure 8.2:**  $\mathbf{k}$  space description of modes. Every positive triplet of integers  $r, s, t$  defines a unique mode. We can thus associate a primitive volume  $\pi^3/abc$  in  $\mathbf{k}$  space with each mode.

To find the total number of modes with  $\mathbf{k}$  values between 0 and  $k$ , we divide the corresponding volume in  $\mathbf{k}$  space by the volume per mode:

$$N(k) = \frac{\left(\frac{1}{8}\right) \frac{4\pi}{3} k^3}{\frac{\pi^3}{V}} = \frac{k^3 V}{6\pi^2} \quad (8.2.13)$$

(The factor  $1/8$  is due to the restriction of  $r, s, t > 0$ .) We next use (8.2.12) to obtain the number of modes with resonant frequencies between 0 and  $\nu$ :

$$N(\nu) = \frac{4\pi\nu^3 n^3 V}{3c^3} \quad (8.2.14)$$

The mode density, that is, the number of modes per unit  $\nu$  near  $\nu$  in a resonator with volume  $V (\gg \lambda^3)$ , is thus

$$p(\nu) = \frac{dN(\nu)}{d\nu} = \frac{8\pi\nu^2 n^3 V}{c^3} \quad (8.2.15)$$

where we multiplied the final result by 2 to account for the two independent orthogonally polarized modes that are associated with each  $r, s, t$  triplet.

The number of modes that fall within the interval  $d\nu$  centered on  $\nu$  is thus

$$N \simeq \frac{8\pi\nu^2 n^3 V}{c^3} d\nu \quad (8.2.16)$$

where  $V$  is the volume of the resonator.

**Example: Number of modes in a typical laser resonator**

For the case of  $V = 1 \text{ cm}^3$ ,  $\nu = 3 \times 10^{14} \text{ Hz}$  and  $d\nu = 3 \times 10^{10}$ , as an example, (8.2.16) yields  $N \sim 2 \times 10^9$  modes. If the resonator were closed, all these modes would have similar values of  $Q$ . This situation is to be avoided in the case of lasers, since it will cause the atoms to emit power (thus causing oscillation) into a large number of modes, which may differ in their frequencies as well as in their spatial characteristics .

This objection is overcome to a large extent by the use of open resonators, which consist essentially of a pair of opposing flat or curved reflectors. In such resonators the energy of the vast majority of the modes does not travel at right angles to the mirrors and will thus be lost in essentially a single traversal. These modes will consequently possess a very low  $Q$ . If the mirrors are curved, the few surviving modes will, as shown below, have their energy localized near the axis; thus the diffraction losses caused by the open sides can be made small compared with other loss mechanisms such as mirror transmission.

### 8.3 Fundamental laser linewidth <sup>3</sup>

#### The Phase Noise

An ideal monochromatic radiation field can be written as

$$\mathfrak{E}(t) = \text{Re}[E_0 e^{i(\omega_0 t + \theta)}] \quad (8.3.1)$$

where  $\omega_0$  the radian frequency,  $E_0$  the field amplitude, and  $\theta$  are constants. A real field including that of lasers undergoes random phase and amplitude fluctuations that can be represented by writing

$$\mathfrak{E}(t) = \text{Re}[E(t) e^{i(\omega_0 t + \theta(t))}] \quad (8.3.2)$$

where  $E(t)$  and  $\theta(t)$  vary only “slightly” during one optical period.

There are many reasons in a practical laser for the random fluctuation in amplitude and phase. Most of these can be reduced, in theory, to inconsequence by various improvements such as ultra-stabilization of the laser cavity length and the near elimination of microphonic and temperature variations. There remains, however, a basic source of noise that is quantum mechanical in origin. This is due to spontaneous emission that continually causes new power to be added to the laser oscillation field. The electromagnetic field represented by this new power, not being coherent with the old field, causes phase, as well as amplitude, fluctuations. These are responsible ultimately for the deviation of the evolution of the laser field from that of an ideal monochromatic field, i.e., for the quantum mechanical noise.

Let us consider the effect of one spontaneous emission event on the electromagnetic field of a single oscillating laser mode. A field such as (8.3.1) can be represented by a phasor of length

<sup>3</sup>Chapter 10 (Page 393 - 396) - Optical Electronics in Modern Communications- Fifth Edition - Amnon Yariv - Oxford University Press, 1997

$E_0$  rotating with an angular (radian) rate  $\omega_0$ . In a frame rotating at  $\omega_0$  we would see a constant vector  $E_0$ . Since  $E_0^2 \propto \bar{n}$ , the average number of quanta in the mode, we shall represent the laser field phasor before a spontaneous emission event by a phasor of length  $\sqrt{\bar{n}}$  as in Figure 8.3. The spontaneous emission adds *one* photon to the field, and this is represented, according to our conversion, by an incremental vector of unity length. Since this field increment is not correlated in phase with the original field, the angle  $\phi$  is a random variable. (i.e., it is distributed uniformly between zero and  $2\pi$ ). The resulting change  $\Delta\theta$  of the field phase can be approximated for  $\bar{n} \gg 1$  by

$$\Delta\theta_{\text{one emission}} = \frac{1}{\sqrt{\bar{n}}} \cos \phi \quad (8.3.3)$$

Next consider the effect of  $N$  spontaneous emissions on the phase of the laser field. The problem is one of random walk, since  $\phi$  may assume with equal probability any value between 0 and  $2\pi$ . We can then write

$$\langle [\Delta\theta(N)]^2 \rangle = \langle (\Delta\theta_{\text{one emission}})^2 \rangle N \quad (8.3.4)$$

and from (8.3.3)

$$\langle [\Delta\theta(N)]^2 \rangle = \frac{1}{\bar{n}} \langle \cos^2 \phi \rangle N \quad (8.3.5)$$

where  $\langle \rangle$  denotes an ensemble average taken over a very large number of individual emission events.

Equation (8.3.4) is a statement of the fact that in a random walk problem the mean squared distance traversed after  $N$  steps is the square of the size of one step times  $N$ . The mean deviation  $\langle \Delta\theta(N) \rangle$  after  $N$  spontaneous emissions is, of course, zero. Any one experiment, however, will yield a nonzero result. The mean squared deviation is thus nonzero and is a measure of the phase fluctuation. To obtain the root-mean-square (rms) phase deviation in a time  $t$ , we need to calculate the average number of spontaneous emission events  $N(t)$  into a single laser mode in a time  $t$ .

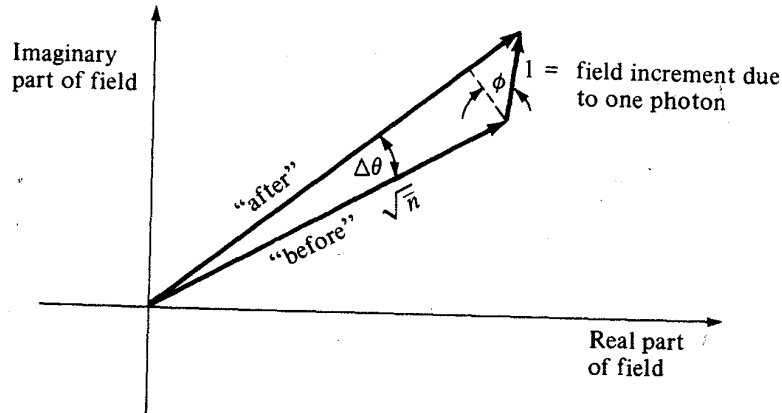


**Figure 8.3:** The phasor model for the effect of a single spontaneous emission event on the laser field phase.

The total number of spontaneous transitions per second into all modes is  $N_2/t_{\text{spont}}$ , where  $N_2$  is the total number of atoms in the upper laser level 2 and  $t_{\text{spont}}$  is the spontaneous lifetime of an atom in 2. The total number of transitions per second into one mode is thus

$$\frac{N_{\text{spont}}}{\text{second-mode}} = \frac{N_2}{t_{\text{spont}} p} \quad (8.3.6)$$

where

$$p = \frac{8\pi\nu_0^2 \Delta\nu V n^3}{c^3} \quad (8.3.7)$$

is the number of modes interacting with the laser transition, i.e., partaking in the spontaneous emission.  $V$  is the mode volume, and  $\Delta\nu$  is the line width of the atomic transition responsible for the laser gain. We can rewrite (8.3.7) as

$$\frac{N_{\text{spont}}}{\text{second-mode}} = \left( \frac{N_2}{\Delta N_t} \right) \frac{(\Delta N_t)}{t_{\text{spont}} p} \quad (8.3.8)$$

where  $\Delta N_t$  is the population inversion ( $N_2 - N_1$ ) at threshold.

$$\Delta N_t = \frac{pt_{\text{spont}}}{t_c} \quad (8.3.9)$$

where  $t_c$  is the photon lifetime in the resonator, and obtain

$$\frac{N_{\text{spont}}}{\text{second-mode}} = \frac{\mu}{t_c} \quad \mu \equiv \frac{(N_2)_t}{\Delta N_t} = \frac{(N_2)_t}{(N_2 - N_1)_t} \quad (8.3.10)$$

The number of spontaneous transitions into a single mode in a time  $\tau$  is thus

$$N(\tau) = \frac{\mu\tau}{t_c} \quad (8.3.11)$$

We recall here that in an ideal four-level laser  $N_1 = 0$  and  $\Delta N_t = N_2$  i.e.  $\mu = 1$ . In a three-level laser, on the other hand,  $\mu$  can be appreciably larger than unity. In a ruby laser at room temperature, for example,  $\mu \approx 50$ . This reflects the fact that for a given gain the total excited population  $N_2$  of a three-level laser must exceed that of a four-level laser by the factor  $f.L$ , since gain is proportional to  $N_2 - N_1$ . Equation (8.3.10) is also equivalent to stating that above threshold there are  $\mu$  spontaneously emitted photons present in a laser mode.

Using (8.3.11) in (8.3.5), we obtain for the root-mean-square phase deviation after  $\tau$  seconds

$$\Delta\theta(t) \equiv \langle [\Delta\theta(N)]^2 \rangle^{1/2} = \sqrt{\frac{1}{2\bar{n}} \frac{\mu t}{t_c}} \quad (8.3.12)$$

The maximum time  $t$  available for such an experiment is the integration time  $T$  of the measuring apparatus so that

$$\Delta\theta(T) = \sqrt{\frac{1}{2\bar{n}} \frac{\mu T}{t_c}} \quad (8.3.13)$$

The rms frequency excursion caused by  $\Delta\theta$  is

$$(\Delta\omega)_{RMS} = \frac{\Delta\theta(T)}{T} \Delta\theta(T) = \sqrt{\frac{\mu}{2\bar{n}t_c T}} \quad (8.3.14)$$

We can cast the last result in a more familiar form by using the relations

$$P_e = \frac{\bar{n}\hbar\omega_0}{t_c} \quad B = \frac{1}{2T} \quad (8.3.15)$$

Here  $P_e$  is the power emitted by the atoms (i.e., the sum of the useful power output plus any power lost by scattering and absorption), and  $B$  is the bandwidth in hertz of the phase-measuring apparatus. The result is

$$(\Delta\omega)_{RMS} = \frac{\Delta\theta(T)}{T} \Delta\theta(T) = \sqrt{\frac{\mu\hbar\omega_0}{P_e t_c^2} B} \quad (8.3.16)$$

From the experimental point of view  $(\Delta\omega)_{RMS}$  is the root-mean-square deviation of the reading of an instrument whose output is the frequency  $\omega(t) = d\theta/dt$ . We will leave it as an exercise for the student to design an experiment that measures  $(\Delta\omega)_{RMS}$ .

Ring laser gyroscopes sense rotation by comparing the oscillation frequencies of two counter-propagating modes in a rotating ring resonator. Their sensitivity, i.e., the smallest rotation rate that they can sense, is thus limited by any uncertainty  $\Delta\omega$  in the laser frequency. Experiments have indeed demonstrated a rotation measuring sensitivity approaching the quantum limit as given by (8.3.16).

[At the end it is also should be mentioned that it is conventional to write  $(\Delta\omega)_{RMS}$  in form of spectral density with the following definition:

$$S(\Omega) \equiv \frac{\Delta\omega_{RMS}^2}{B} = \left( \frac{\mu\hbar\omega_0}{P_e t_c^2} \right) \quad (8.3.17)$$

In Figure 8.4 one can find the Typical spectral density of a diode laser ] <sup>4</sup>

<sup>4</sup>This part is added by authors

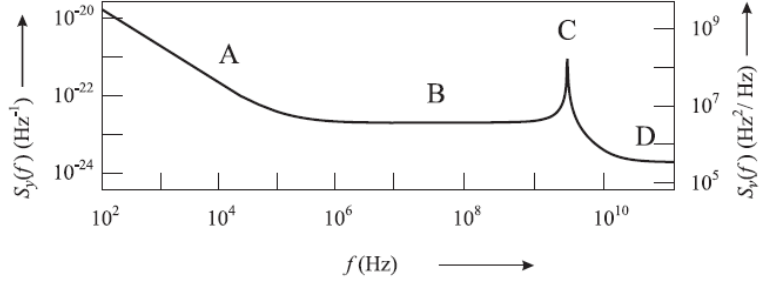


**Figure 8.4:** Typical power spectral densities  $S_y(f)$  and  $S_{\nu}(f)$  of a diode laser near 850 nm as function of the Fourier frequency  $f$  according to with different regimes. A:  $1/f$  fluctuations. B: fluctuations of the carrier density. C: relaxation oscillations. D: fluctuation of the spontaneous emission.

## 8.4 The random intensity noise<sup>5</sup>

### Intensity Noise

Spontaneous emission causes laser radiation to have random fluctuations in *power* as well as phase. Thus, the output power of a single-mode laser is described by

$$P(t) = P_{\text{out}} + \Delta P(t) \quad (8.4.1)$$

$P_{\text{out}}$  is the average output power and  $\Delta P(t)$  is the fluctuation at time  $t$  of the power from its average value. As usual  $\langle X \rangle$  denotes the average over the ensemble of all possible values of  $X$ . We will assume that the “random process”  $\Delta P(t)$  is stationary and ergodic, so that  $\langle \Delta P(t) \Delta P(t + \tau) \rangle$  is independent of  $t$  and ensemble averages are equal to time averages .

A conventional measure of power fluctuations is the *relative intensity noise* (RIN)

$$\text{RIN}(\omega) = \frac{S_p(\omega)}{P_{\text{out}}^2} \quad (8.4.2)$$

where the spectral power density  $S_p(\omega)$  is defined in this context as the Fourier transform of the autocorrelation function  $\langle \Delta P(t) \Delta P(t + \tau) \rangle$ :

$$S_p(\omega) = \int_{-\infty}^{\infty} \langle \Delta P(t) \Delta P(t + \tau) \rangle e^{-i\omega\tau} d\tau \quad (8.4.3)$$

From the inverse Fourier transform of (8.4.4) we have<sup>6</sup>

$$\langle \Delta P(t) \Delta P(t + \tau) \rangle = \frac{1}{2\pi} \int_{-\infty}^{\infty} S_p(\omega) e^{i\omega\tau} d\omega \quad (8.4.4)$$

and in particular the relative mean-square power fluctuation is

$$\begin{aligned} \frac{\langle \Delta P^2 \rangle}{P_{\text{out}}^2} &= \frac{\langle [P(t) - P_{\text{out}}]^2 \rangle}{P_{\text{out}}^2} = \frac{\langle \Delta P(t) \Delta P(t) \rangle}{P_{\text{out}}^2} = \frac{1}{2\pi P_{\text{out}}^2} \int_{-\infty}^{\infty} S_p(\omega) d\omega \\ &= \frac{1}{2\pi} \int_{-\infty}^{\infty} \text{RIN}(\omega) d\omega \end{aligned} \quad (8.4.5)$$

from which we can define a laser signal-to-noise ratio:

$$SNR_L = \sqrt{\frac{P_{\text{out}}^2}{\langle \Delta P^2 \rangle}} = \frac{\sqrt{2\pi}}{\sqrt{\int_{-\infty}^{\infty} \text{RIN}(\omega) d\omega}} \quad (8.4.6)$$

<sup>5</sup>Chapter15 (Pages 771 - 772) - Laser Physics - Peter W. Milonni, Joseph H. Eberly - Hoboken, New Jersey : John Wiley & Sons Ltd, 2010

<sup>6</sup>The fact that the spectral density and the autocorrelation function are Fourier transforms of each other is the WienerKhinchine theorem.

## 8.5 Laser gyroscope and the fundamental linewidth; sensitivity estimate <sup>7</sup>

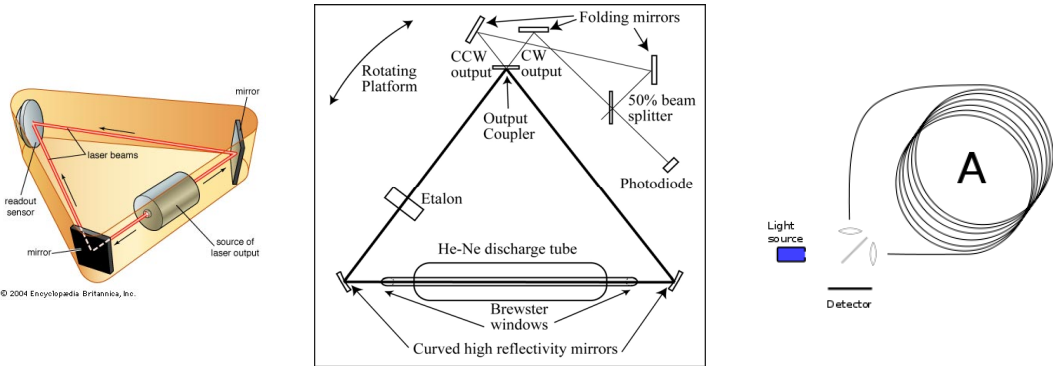


**Figure 8.5:** Three types of Gyroscope.

The toy gyroscope sketched in Figure 8.6 demonstrates an important property of a mechanical gyroscope: the axis about which the wheel spins maintains its direction when the frame of the gyroscope is tilted. A gyroscope on a ship likewise maintains its orientation as the ship rolls in rough water, and thereby provides information on the degree of roll. Gyroscopes are also used on aircraft as compasses and in automatic pilot systems, in torpedoes for steering to the target, and for the inertial guidance of missiles. In a sense the earth itself is a kind of gyroscope: its rotation axis maintains its orientation as the earth orbits about the sun. It is this fixed orientation, of course, that is responsible for changes of season.

In general we can define a gyroscope as a device capable of sensing angular velocity: indeed the word gyroscope itself means “viewing rotation”. A gyroscope therefore need not have a spinning wheel, nor need it be a purely mechanical instrument. In this section we will describe how a ring laser may be used to sense angular velocity, or in other words how it may be used as a gyroscope.

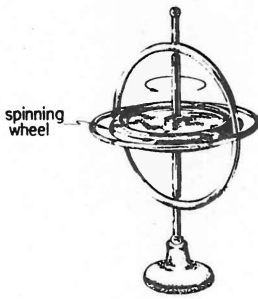


**Figure 8.6:** A mechanical gyroscope. The axis about which the wheel spins stays fixed as the frame of the gyroscope is rotated.

First let us consider a thought experiment in which we have somehow managed to get two monochromatic waves propagating in a circular path of radius  $R$ , one propagating clockwise and the other counterclockwise, as illustrated in Figure 8.7a. The time taken to complete the circular path of circumference  $2\pi R$  is

$$t = \frac{2\pi R}{c} \quad (8.5.1)$$

This transit time is the same for the two counterpropagating waves.

Suppose, however, that the plane of the circular path is rotating with angular velocity  $\Omega$ , as in Figure 8.7b. In this case a point  $A$  on the circle is moving with tangential velocity  $\nu = \Omega R$ . The

---

7 Chapter 16 (Page 589 - 594) - Lasers - Peter W. Milonni, Joseph H. Eberly - New York [etc.] : Wiley, cop. 1988

light propagating in the same sense as the rotation takes a time  $t_+$ , to go from point  $A$  to point  $B$  in Figure 8.7b, where

$$2\pi R + (\Omega R)t_+ = ct_+ \quad (8.5.2)$$

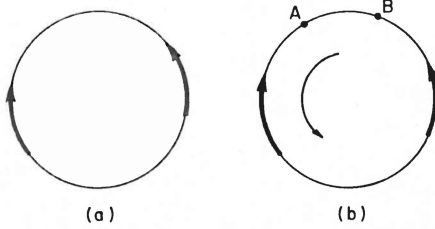


**Figure 8.7:** (a) A thought experiment in which two waves propagate on a circular loop. one clockwise and the other counterclockwise. (b) The case in which the plane or the circular loop is rotating. In this case the two waves take different amounts of time to transverse the arc between two points  $A$  and  $B$ .

$$t_+ = \frac{2\pi R}{c - \Omega R} \quad (8.5.3)$$

The left side of (8.5.2) is the circumference of the circle plus the distance along the circle between points  $A$  and  $B$ . Thus  $t_+$  is greater than the transit time (8.5.1) when there is no rotation, because during the transit time of the light the reference point  $A$  moves from  $A$  to  $B$ , and so the light must travel the extra distance  $\Omega R t_+$  to complete a round trip as reckoned by an observer at rest on the circle. The light propagating in the sense opposite to the rotation, however, takes a shorter time,  $t_-$ , to complete a round trip:

$$2\pi R - (\Omega R)t_- = ct_- \quad (8.5.4)$$

or

$$t_- = \frac{2\pi R}{c + \Omega R} \quad (8.5.5)$$

According to an observer sitting at a point on the circle, therefore, the two waves have gone different distances in making a round trip: their path difference is

$$\begin{aligned} \Delta L &= c(t_+ - t_-) = 2\pi R c \left( \frac{1}{c - \Omega R} - \frac{1}{c + \Omega R} \right) \\ &= 2\pi R c \frac{2\Omega R}{c^2 - \Omega^2 R^2} \\ &\approx \frac{4\pi R^2 \Omega}{c} \end{aligned} \quad (8.5.6)$$

where the approximation in the last step is based on the assumption that the tangential velocity of a point on the circle is much less than the velocity of light (i.e.  $\Omega R \ll c$ ).

The path difference (8.5.6) corresponds to a phase difference

$$\begin{aligned} \Delta\phi &= 2\pi \frac{\Delta L}{\lambda} = \frac{8\pi^2 R^2 \Omega}{\lambda c} \\ &= \frac{8\pi A \Omega}{\lambda c} \end{aligned} \quad (8.5.7)$$

where  $A = \pi R^2$  is the area enclosed by the circular loop. Actually (8.5.7) is the correct result (to first order in  $v/c$ ) for a closed loop of *any* shape. For instance, it applies to the three-mirror ring arrangement shown in Figure 8.8. And so we can forget the artificial constraints of our thought experiment with a circular loop and consider such a triangular ring, for example. By measuring interferometrically the phase difference  $\Delta\phi$ , between two counterpropagating light beams at a fixed point on the ring, we can measure the angular velocity  $\Omega$ . In other words, we can make an *optical gyroscope*.<sup>8</sup>

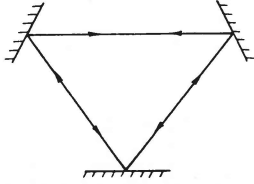


**Figure 8.8:** A three-mirror ring forming a closed loop for the propagation of light. Equation (8.5.7) applies to any such closed loop, whether it is a circle, triangle, square, etc.

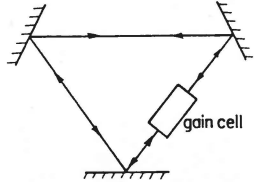


**Figure 8.9:** A three-mirror ring laser that can be used as an optical gyroscope.

The ability to sense rotation in this way is called the *Sagnac effect*, after George Sagnac, who in 1913 first demonstrated it using a rapidly rotating table. The main difficulty in using a “Sagnac interferometer” as a gyroscope is that the phase shift  $\Delta\phi$ , is typically very small, because the path difference  $\Delta L$  of the counterpropagating waves is small compared with the wavelength  $\lambda$ . After Sagnac’s demonstration Michelson used about 5 miles of (evacuated) sewer pipes to construct a Sagnac interferometer for detecting the earth’s rotation. Without large loop areas ( $A$ ) or large angular velocities ( $\Omega$ ), the phase shift (8.5.7) is too small to be measured accurately.

Suppose we put a gain cell inside the three-mirror resonator of Figure 8.8 to make a ring laser (Figure ??). In this case the two counterpropagating beams required for the Sagnac interferometer are generated by laser action inside the gain cell. Like the ordinary two-mirror, linear laser resonator, the ring resonator must satisfy the condition that the total round-trip distance  $L$  must be equal to an integral number  $m$  of wavelengths, or in other words

$$\nu = mc/L \quad (8.5.8)$$

In particular, a small change  $\Delta L$  in  $L$  results in a change  $\Delta\nu$  in  $\nu$  given by

$$\Delta\nu = \frac{\nu\Delta L}{L} = \frac{c\Delta L}{\lambda L} \quad (8.5.9)$$

Unlike a linear laser resonator, however, the two counterpropagating waves in a ring laser need not have the same frequency. In fact, if the ring is rotating about an axis perpendicular to its plane, the two waves “see” different round-trip distances  $L_+ = ct_+$  and  $L_- = ct_-$ , and they will have a frequency difference (8.5.9) with  $\Delta L$  given by (8.5.6). That is, the two counterpropagating waves in a rotating ring laser have the frequency difference

$$\begin{aligned} \Delta\nu &= \frac{c}{\lambda L} \left( \frac{\lambda}{2\pi} \Delta\phi \right) \\ &= \frac{c}{2\pi L} \left( \frac{8\pi A\Omega}{\lambda c} \right) \\ &= \frac{4A\Omega}{\lambda L} \end{aligned} \quad (8.5.10)$$

where  $\Omega$  is the angular velocity of rotation and  $A$  is the area enclosed by the ring of perimeter  $L$ .

<sup>8</sup>See Dana Z. Anderson. "Optical Gyroscopes." *Scientific American* 254, April 1986, p. 94.

**Example: Frequency shift for a an optical gyroscope in earth rotation.**

Let us consider a numerical example. For a ring resonator of the type shown in Figure 8.8 with side  $d = 10$  cm, we have  $A = \sqrt{3}d^2/4 \approx 43.3$  cm<sup>2</sup> by simple geometry. If the angular velocity  $\Omega = 15$  deg/hr =  $7.3 \times 10^{-5}$  rad/sec. the rotation rate of the Earth, then (8.5.7) gives

$$\Delta\phi = 4.2 \times 10^{-8} \text{ rad} \quad (8.5.11)$$

for the He-Ne laser wavelength  $\lambda = 6328\text{\AA}$ . This corresponds to a ratio  $\Delta L/\lambda = \Delta\phi/2\pi = 6.7 \times 10^{-9}$ , and so for this loop area and rotation rate the measurement of  $\Delta\phi$ , is a formidable task indeed. From (8.5.10) for the ring laser gyro, on the other hand, we compute for the same parameters

$$\Delta\nu = 20 \text{ Hz} \quad (8.5.12)$$

which is readily measured by optical heterodyning. even though it represents a tiny fraction ( $\approx 4 \times 10^{-14}$ ) of the optical frequency  $\nu$ .

A great advantage of laser gyroscopes, as compared with conventional spinning- mass gyros, is that they have no moving parts to produce mechanical stress and wear. They can furthermore be operated. in the “strapped-down mode” in which they are rigidly fixed to a vehicle without any gimbals. Laser-gyro construction is relatively simple and inexpensive. Typically the ring resonator and a He-Ne gain tube are enclosed in a single drilled-out quartz block small enough to be held in one’s hand. Attached to the block is the “readout” apparatus, which uses a partially transmitting mirror to combine parts of the two counterpropagating beams and measure their frequency difference interferometrically. For navigational purposes the measured rotation rate is integrated to give the total angle of rotation over a given time.

A problem with laser gyroscopes is called *lock-in*. It occurs at low rotation rates, and causes low beat frequencies to tend to lock together at a *single* intermediate frequency. (This locking phenomenon often arises in coupled oscillatory systems.) Lock-in obviously destroys the ability to measure small rotation rates. One technique used to alleviate the lock-in problem is to “dither” the gyro, i.e., to rotate it back and forth rapidly enough that lock-in cannot occur. On average the back and forth motions cancel, and what is left after a number of dithering periods is just the rotation rate one wants to measure.

Laser gyroscopes are now used on commercial airliners, and several nations are using them in military vehicles. Another type of optical rotation sensor that uses the same principles of operation is based on an optical fiber loop instead of a ring laser to form a Sagnac interferometer.

